Letter

Hydrodynamic scaling of metachronal swimming

Kuvvat Garayev and David W. Murphy*
Department of Mechanical Engineering, University of South Florida, Tampa, Florida 33620, USA

(Received 29 June 2022; accepted 20 September 2024; published 4 November 2024)

Metachronal swimming consists of the sequential stroking of multiple appendages or cilia, resulting in a wave of appendage motion traveling along the body. Further, metachronal swimming spans the viscous to inertial regimes as it is used across seven orders of magnitude of Reynolds numbers Re_b, where $\mathrm{Re}_b = VL/\nu$, and V, L, and ν are the characteristic swimming speed, body length, and fluid kinematic viscosity, respectively. Through analysis of morphological and kinematics data collected from the literature on a wide variety of metachronally swimming organisms, we examine how these factors affect swimming performance across Re_b. Further, we find a strong relationship among the kinematics parameters, swimming speed, and fluid viscosity. This power law relationship, $\mathrm{Re}_b \sim Sw$, where $Sw = \omega AL/\nu$ is the Swimming number (ω: average angular appendage tip speed, A: appendage tip excursion), is maintained for all flow regimes, explains why metachronal swimming is a successful locomotion mode at low Reynolds numbers, and may prove useful in designing bio-inspired robots. We also find that the Strouhal number $St = fA/V$, where f is beat frequency, is relatively constant across a wide range of Re_b but suggest that Sw better describes the underlying hydrodynamics of metachronal swimming.

DOI: 10.1103/PhysRevFluids.9.L111101

Introduction. Metachronal swimming is a ubiquitous locomotion mode occurring in organisms with multiple appendages or cilia that undergo sequential beating (i.e., rowing) [1,2]. This form of locomotion is used by approximately 17% of the global marine biomass across a wide variety of invertebrate taxa including crustaceans, ctenophores, tomopterids, and paramecia. Indeed, the global biomass of a single metachronally swimming species (the Antarctic krill *Euphausia superba*) approximately equals the global human biomass [3,4]. For comparison, fish swimming moves only 12% of marine biomass [5,6]. Most metachronally swimming animals use an antiplectic pattern, in which the power stroke direction is opposite to the appendage wave direction, though other patterns also occur in ciliated organisms [1,7]. Metachronal swimmers range in size approximately from 0.1 mm to 0.1 m. While metachronal swimming is observed in all flow regimes (viscous to inertial), most metachronal swimmers operate in the intermediate Re_b regime ($1 < \mathrm{Re}_b < 1000$), where both viscous and inertial forces play a significant role [Fig. 1(a)]. Thus, the simplifying assumptions used to solve the Navier-Stokes equations at low ($\mathrm{Re}_b \leqslant 1$) and high Re_b ($\mathrm{Re}_b \geqslant 1000$) flow regimes are not valid [7]. At low Re_b, the flow is reversible and primarily governed by viscous forces, and thus analytical solutions exist; at high Re_b, flow is mainly governed by inertial forces, and thus potential flow approximations can be utilized [7].

Hydrodynamics-based scaling relationships that link body kinematics and fluid properties to swimming speed are useful in predicting the performance of a swimmer under specified kinematics and may be useful in designing bio-inspired robots [8–10]. For undulatory aquatic locomotion [11] performed a scaling analysis and developed a relationship between a novel Swimming Number Sw

*Contact author: davidmurphy@usf.edu

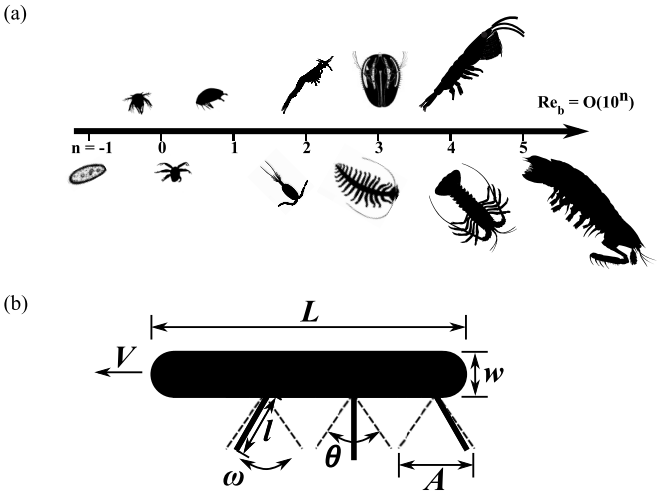

FIG. 1. (a) Metachronal swimmers considered in this study span seven orders of magnitude in Reynolds number and include ciliates (e.g., paramecia), barnacle larvae, copepods (larvae and adult), mysid shrimp, tomopterid worms, ctenophores, lobsters, krill, and mantis shrimp (Refs. for species silhouettes are given in [6]). (b) Cartoon of a metachronal swimmer with three appendage pairs ($n = 6$) showing important morphological and kinematic parameters.

and Re_b. Here, $Sw = \frac{\omega A L}{\nu}$ is a transverse Reynolds number characterizing the tail motion that drives the animal, where A and ω are tail tip excursion and angular speed, respectively. A wide range of aquatic animals, including fish, mammals, reptiles, and invertebrate larvae, were found to obey a $\mathrm{Re}_b \sim Sw^{4/3}$ relationship below $\mathrm{Re}_b = 3000$ and a $\mathrm{Re}_b \sim Sw$ relationship above $\mathrm{Re}_b = 3000$. This difference in scaling is explained by the fact that swimmers in the laminar regime experience relatively higher levels of viscous drag in comparison to high Re_b swimmers in the turbulent regime. However, no such unifying relationship exists for metachronal swimmers. One reason for this is the morphological complexity of metachronal swimmers as compared to undulatory swimmers. Whereas undulatory swimmers may be characterized by a single length scale (e.g., body length), metachronal swimmers are characterized by multiple length scales (e.g., body and appendage length) and have different numbers of propulsors. Further, metachronal swimmers have a wide range of body shapes and appendage insertion locations, ranging from almost spherical ctenophores with appendages distributed across the body to highly elongated tomopterid worms with appendages distributed laterally along the body length. This morphological complexity does not easily lend itself to a simple scaling analysis. Here we examine the range of metachronal swimmer morphologies, identify a Swimming Number analogous to that identified by [11] for undulatory swimmers, and examine the resulting scaling relationships.

Methods. Figure 1(b) shows a cartoon of a metachronal swimmer with n number of appendages, body length L, body width w, appendage length l, constant swimming speed V, appendage beat frequency f, and appendage stroke amplitude θ (in units of radians). Figure 1(b) shows the body of a crustacean-type metachronal swimmer (e.g. shrimp) as a stadium (i.e., a rectangle with two half-circles on the ends) with multiple appendage pairs ($n = 6$) located ventrally. We collect morphological and swimming kinematics data from the literature for various metachronal swimmers with $n > 2$, including paramecia, ctenophores, crustaceans, tomopterid worms, and a krill-inspired "Krillbot" robot [9,12–34]. Based on these data, we investigate morphological patterns, calculate Re_b and Sw, and examine scaling relationships. For comparison, these data are also collected and calculations are made for organisms such as cladocerans, which swim by rowing a single

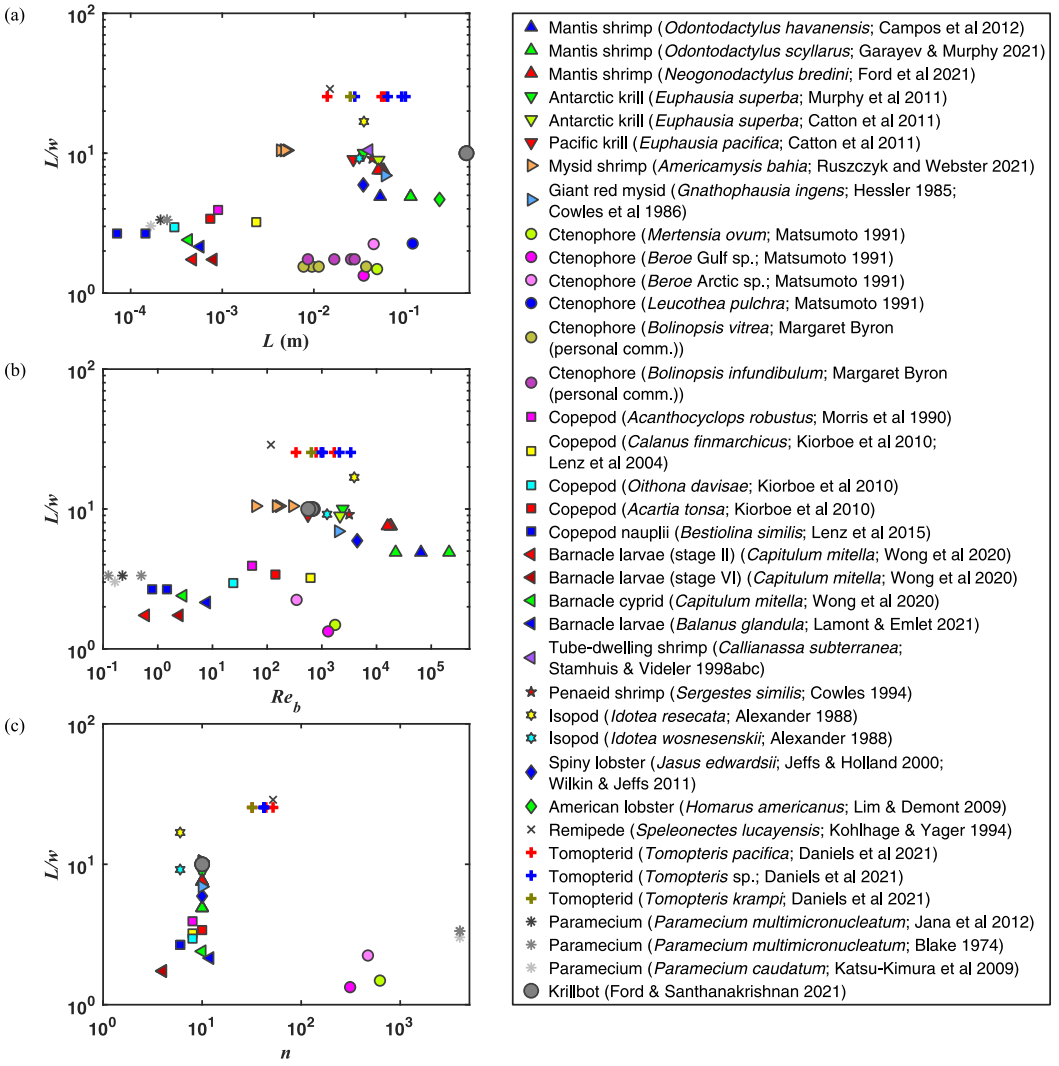

FIG. 2. Plots of L/w vs L (a), L/w vs Re_b (b), and L/w vs n (c) for metachronal swimmers considered in this study. The ratio of L/w is measured either from images in the studies cited in Fig. 2 or from various online sources.

pair ($n = 2$) of appendages [35–38]. See Supplemental Material [6,39] for the collected data and calculations.

Results and discussion. We first consider the variation in body plan among metachronal swimmers and its relation to body length, Reynolds number, and number of appendages. Figs. 2(a) and 2(b) show how the ratio L/w, which describes the animal's aspect ratio, varies with body length L and body Reynolds number Re_b. Figs. 2(a) and 2(b) show that the smallest animals swimming at the lowest Re_b (e.g., paramecia, copepods, and various zooplankton larvae) consistently have low values of L/w, a body plan consistent with a need to minimize viscous drag, which dominates at these Reynolds numbers. In contrast, larger animals (e.g., $L >\sim 10^{-2}$ m) have a wide variety of body shapes, from elongated tomopterids to almost-spherical ctenophores [Fig. 2(a)]. However, metachronally swimming animals with $L/w <\sim 5$ are absent for $\mathrm{Re}_b >\sim 2000$, indicating body plan streamlining becomes important at these higher Reynolds numbers at which pressure drag

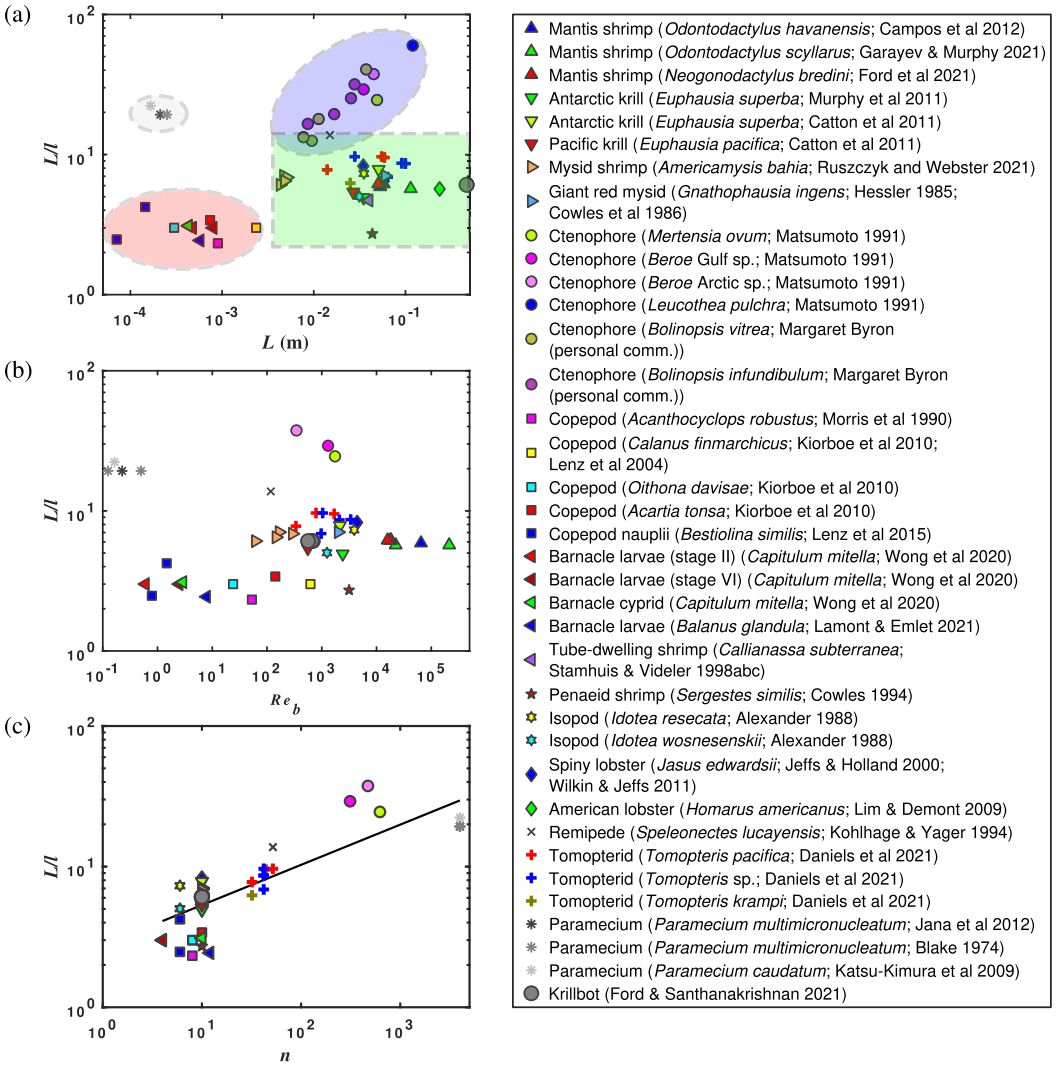

FIG. 3. Metachronal swimmers possess a variety of shapes, sizes, Reynolds numbers, and leg numbers. Plots of L/l vs L (a), L/l vs Re_b (b), and L/l vs n (c) for organisms as diverse as crustaceans, tomopterids, ctenophores, and paramecia. For the plot of L/l vs n, a power law fit yields $L/l = 2.8(n)^{0.3}$ with $R^2 = 0.57$. Krillbot data are not included in the regression.

dominates (Fig. 2). Finally, Fig. 2(c) shows that there is not a strong relationship between L/w and n, which seems largely to be determined by phylogeny (e.g., most metachronally swimming crustacean species have 4–5 appendage pairs (see Fig. S2 of the SM [6]).

We next consider how the relative size of the thrust-producing appendages varies with the body length, Reynolds number, and number of appendages among metachronal swimmers. Figures 3(a) and 3(b) show that L/l varies across two orders of magnitude and largely clusters into four groups [indicated in Fig. 3(a)] loosely based on phylogeny. First, paramecia, which are quite small and swim at $\mathrm{Re}_b < 1$, have small appendages relative to their body size ($L/l =\sim 20$). Second, ctenophores are much larger and swim much faster ($100 < \mathrm{Re}_b < 1000$), but also have small appendages relative to their body size ($L/l > 20$) [40]. Large values of L/l for both paramecia and ctenophores make sense as both use cilia for propulsion. Third, copepods and various zooplankton larvae are generally small

($L <\sim 10^{-3}$ m), swim at $\mathrm{Re}_b <\sim 10^2$, and have large appendages relative to their body size ($L/l = \sim 2{-}4$). Fourth, the larger crustaceans (e.g., krill and shrimp) and tomopterids ($L >\sim 10^{-2}$ m) swim at $\mathrm{Re}_b >\sim 10^2$ and have appendages of intermediate length relative to their body size ($L/l =\sim 4{-}10$). Finally, Fig. 3(c) shows that metachronal swimmers with appendages which are short relative to their body length (e.g., ctenophores and paramecia) tend to have more such appendages [29,41] whereas those with relatively long appendages have only a few appendage pairs (e.g., krill). This relationship between the number and relative size of appendages indicates the existence of different strategies for thrust production (e.g., large numbers of short appendages vs. a small number of long appendages). It is interesting to note that neither of these strategies is restricted to a particular Reynolds number range. For example, both ctenophores (high Re_b) and paramecia (low Re_b) use a strategy with a large number of short ciliary appendages while both krill (high Re_b) and copepods (low Re_b) use a strategy with a small number of long appendages.

Figure 4(a) shows that metachronal swimmers from a wide phylogenetic spread [6], as well as the Krillbot, obey a $\mathrm{Re}_b \sim Sw$ scaling law for $\mathrm{Re}_b = 10^{-1}{-}10^5$. The species in this plot have as few as 4 (barnacle nauplii) and as many as several thousand (paramecium) appendages, and body lengths range from $<$100 μm (copepod nauplii) to $>$10 cm (peacock mantis shrimp). Plotting Re_b as a function of Sw for both undulatory and metachronal swimmers in Fig. 4(b) shows that metachronal swimmers successfully maintain the $\mathrm{Re}_b \sim Sw$ scaling well below $\mathrm{Re}_b = 3000$. In the laminar regime, metachronal swimmers are thus able to achieve higher swimming speeds than undulatory swimmers. These higher swimming speeds are likely the result of metachronal swimmers' ability to generate large levels of thrust by stroking multiple appendages at relatively lower tip speeds [31], which seems to be a key to the success of this swimming mode. Our finding thus provides support for the theory that paddling appendages, which are often used at low Re_b, are tuned for the high levels of thrust needed for maneuvering and rapid acceleration, whereas undulatory swimming, which is more common at high Re_b, is tuned for high efficiency [2,42]. Synergistic flow interactions among appendages [20,31] and suction thrust induced by appendage bending [43] may also play a role in generating these high levels of thrust in metachronal swimmers. On the other hand, metachronal swimmers are uncommon at $\mathrm{Re}_b > 10^4$ and absent at $\mathrm{Re}_b > 10^5$, likely because using appendages as lift-generating hydrofoils (e.g., penguins [44]) is more efficient than using them as paddles, which generate thrust via drag at these higher Reynolds numbers [2]. We note here that other intrinsic biological and environmental factors unrelated to propulsion (e.g., temperature) may also limit the size and thus the Re_b of metachronally rowing organisms [45]. For rowing organisms using a single ($n = 2$) appendage pair (e.g., cladocerans, see Fig. S1 in SM [6]), Fig. 4(b) shows that the trendline for these animals falls below that of the metachronal swimmers, which again shows the advantage that metachronal rowing with many appendages offers in terms of sustained thrust generation and higher swimming speeds.

It is interesting that a simple power-law relationship exists that fits the biological data so well even without explicitly accounting for variations in the body plan, number of appendages, or appendage spacing. In particular, the appendage spacing relative to appendage length is relatively consistent across a wide variety of species [31], which could promote thrust- or efficiency-enhancing hydrodynamic interactions between appendages [20,46]. However, such hydrodynamic interactions found in other biological locomotion systems generally confer rather small benefits. For example, [47] found that the clap-and-fling mechanism used by fruit flies enhances lift by approximately 5–13%, and [48] found that the same mechanism provided up to 30% of the required lift in parasitoid wasp flight. Similarly, [49] showed that vortex interactions between schooling fish lowered energy costs by approximately 5%. Nonetheless, such flow interactions may be biologically significant for metachronal swimmers and should be investigated further, as should the importance of variations in body plan and number of appendages.

Previous researchers have found that the Strouhal number $St = fA/V$ falls in the narrow range of $0.2 < St < 0.4$ for a wide variety of flying and swimming animals at cruising speeds [50–52]. However, [11] showed that Sw captures the input kinematics better than St and that their $St{-}\mathrm{Re}_b$

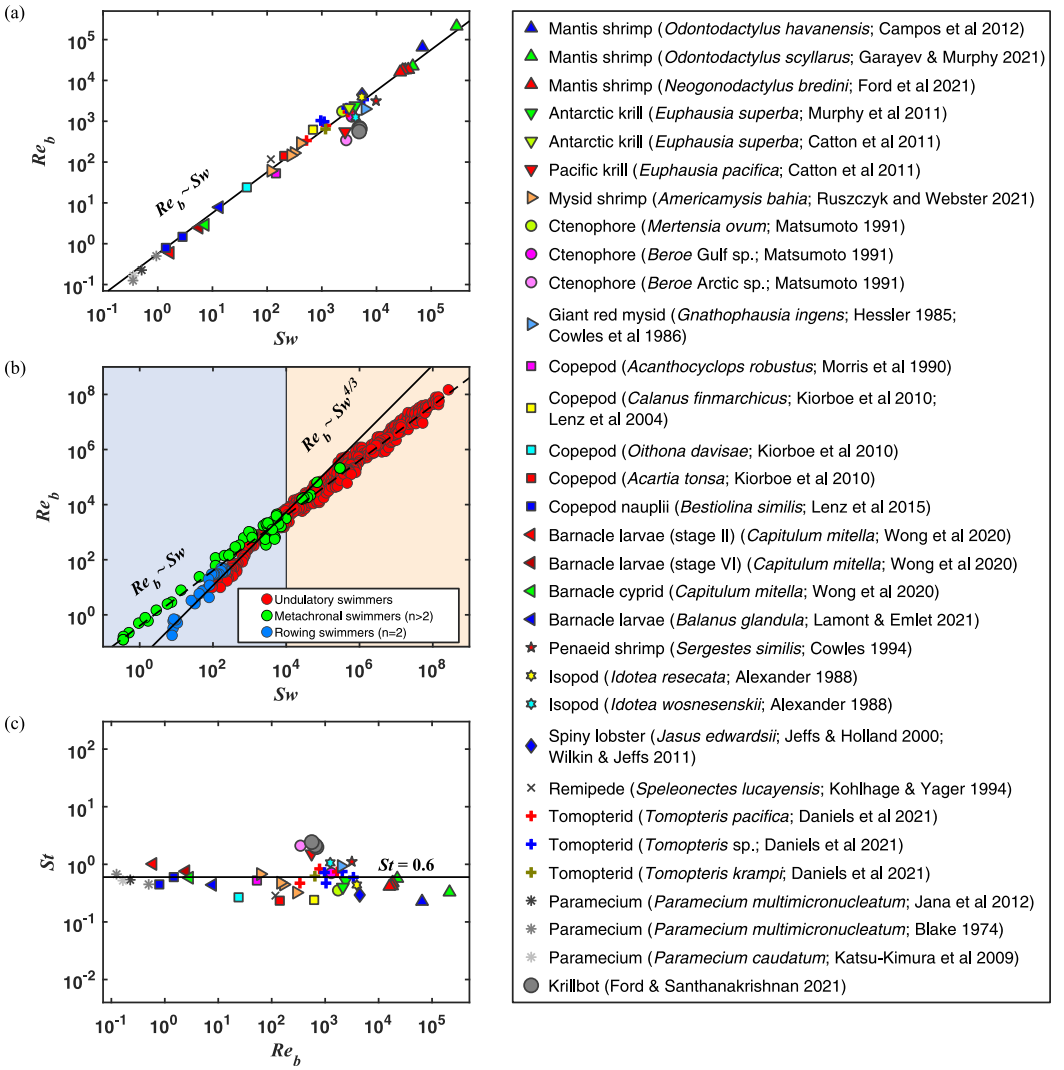

FIG. 4. (a) Re_b plotted vs Sw for a variety of metachronal swimmers. A power law fit yields $\mathrm{Re}_b = 0.5(Sw)^{1.0}$, with $R^2 = 0.99$. (b) Plot of Re_b vs Sw for both undulatory [11], metachronal ($n > 2$), and rowing ($n = 2$) swimmers. (c) St vs Re_b for metachronal swimmers. Species names in (a) and (c) are given in the legend, and references for metachronal and rowing swimmers are provided in the SM [6]). Krillbot data are not included in the regressions.

scaling gives $St \approx 0.3$ for turbulent flows and $St \sim \mathrm{Re}_b{}^{-1/4}$ for laminar flows for undulatory swimmers. For metachronal swimmers, St also is constrained to a limited range of $0.2 < St < 2$, with an average value of $St = 0.6$ across a wide range of Re_b, as shown in Fig. 4(c). Some of the spread in Fig. 4(c) may reflect swimming behaviors other than cruising (e.g., slowly swimming or hovering, which would increase St and decrease Re_b), but it is not unexpected that the range of St would differ for metachronal swimmers as compared to animals employing oscillating, lift-generating hydrofoils or airfoils, since their modes of thrust generation also differ. Nonetheless, we suggest that Sw is a superior descriptor of metachronal swimming hydrodynamics than St, as it better correlates with Re_b and, as noted by [11] for undulatory swimming, accounts for variations

in the fluid viscosity, separates the input appendage kinematics from the output swimming speed, and includes both the appendage and body length scales. We also note that various parameters have been used to characterize the appendage Reynolds number [53,54]. In Fig. S3 of the SM [6], we compare how well these different definitions correlate with Re_b.

Finally, the relationship between Sw and Re_b found here likely represents optimal performance for metachronal swimmers across a wide range of sizes and swimming speeds. Thus, this scaling law may be useful in designing bio-inspired metachronally paddling robots that are optimized for the high levels of thrust generation needed for maneuvering and rapid accelerations. For example, a metachronally swimming prototype which does not reach the Re_b specified by the scaling law for a given value of Sw is underperforming and requires improvement.

Data will be shared on reasonable request to the corresponding author.

Acknowledgments. We are grateful to the National Academies of Science Keck Futures Initiative (NAKFI) and to the National Science Foundation (OPP 1840941) for supporting this work. We thank Dr. Margaret Byron, Dr. Arvind Santhanakrishnan, and Dr. Donald Webster for insightful discussions. We also thank Alina Grossweiner, Dr. Kelly Sutherland, Dr. Sean Colin, and Dr. George Matsumoto for providing ctenophore data.

[1] M. A. Sleigh and D. Barlow, Metachronism and control of locomotion in animals with many propulsive structures, in *Aspects of Animal Movement* (Cambridge University Press, Cambridge, 1980), pp. 49–67.

[2] J. A. Walker and M. W. Westneat, Mechanical performance of aquatic rowing and flying, Proc. R. Soc. London, Ser. B: Biol. Sci. **267**, 1875 (2000).

[3] A. Atkinson, V. Siegel, E. Pakhomov, M. Jessopp, and V. Loeb, A re-appraisal of the total biomass and annual production of Antarctic krill, Deep Sea Res. Part I. **56**, 727 (2009).

[4] Y. M. Bar-On and R. Milo, The biomass composition of the oceans: A blueprint of our blue planet, Cell. **179**, 1451 (2019).

[5] Y. M. Bar-On, R. Phillips, and R. Milo, The biomass distribution on Earth, Proc. Natl. Acad. Sci. **115**, 6506 (2018).

[6] See Supplemental Material at http://link.aps.org/supplemental/10.1103/PhysRevFluids.9.L111101 for details on biomass calculation, data collection for metachronal and single-pair appendage swimmers, references for organism drawings, and phylogenetic trees of species.

[7] T. Daniel, C. Jordan, and D. Grunbaum, Hydromechanics of swimming, Adv. Comp. Environ. Physiol. **11**, 17 (1992).

[8] Y. Cha, J. Laut, P. Phamduy, and M. Porfiri, Swimming robots have scaling laws, too, IEEE/ASME Trans. Mechatron. **21**, 598 (2015).

[9] M. P. Ford and A. Santhanakrishnan, On the role of phase lag in multi-appendage metachronal swimming of euphausiids, Bioinspiration Biomimetics. **16**, 066007 (2021).

[10] S. O. Santos, N. Tack, Y. Su, F. Cuenca-Jiménez, O. Morales-Lopez, P. A. Gomez-Valdez, and M. M. Wilhelmus, Pleobot: a modular robotic solution for metachronal swimming, Sci. Rep. **13**, 9574 (2023).

[11] M. Gazzola, M. Argentina, and L. Mahadevan, Scaling macroscopic aquatic locomotion, Nat. Phys. **10**, 758 (2014).

[12] D. E. Alexander, Kinematics of swimming in two species of Idotea (Isopoda: Valvifera), J. Exp. Biol. **138**, 37 (1988).

[13] J. Blake, Hydrodynamic calculations on the movements of cilia and flagella I. Paramecium, J. Theor. Biol. **45**, 183 (1974).

[14] E. O. Campos, D. Vilhena, and R. L. Caldwell, Pleopod rowing is used to achieve high forward swimming speeds during the escape response of Odontodactylus Havanensis (Stomatopoda), J. Crustacean Biol. **32**, 171 (2012).

[15] K. B. Catton, D. R. Webster, S. Kawaguchi, and J. Yen, The hydrodynamic disturbances of two species of krill: Implications for aggregation structure, J. Exp. Biol. **214**, 1845 (2011).
[16] D. L. Cowles, Swimming dynamics of the mesopelagic vertically migrating penaeid shrimp Sergestes similis: Modes and speeds of swimming, J. Crustacean Biol. **14**, 247 (1994).
[17] D. L. Cowles, J. J. Childress, and D. L. Gluck, New method reveals unexpected relationship between velocity and drag in the bathypelagic mysid Gnathophausia ingens, Deep Sea Res. Part A Oceanogr. Res. Pap. **33**, 865 (1986).
[18] J. Daniels, N. Aoki, J. Havassy, K. Katija, and K. J. Osborn, Metachronal swimming with flexible legs: A kinematics analysis of the midwater polychaete Tomopteris, Integr. Comp. Biol. **61**, 1658 (2021).
[19] M. P. Ford, W. J. Ray, E. M. DiLuca, S. Patek, and A. Santhanakrishnan, Hybrid metachronal rowing augments swimming speed and acceleration via increased stroke amplitude, Integr. Comp. Biol. **61**, 1619 (2021).
[20] K. Garayev and D. W. Murphy, Metachronal swimming of mantis shrimp: Kinematics and interpleopod vortex interactions, Integr. Comp. Biol. **61**, 1631 (2021).
[21] R. R. Hessler, Swimming in crustacea, Earth Environ. Sci. Trans. R. Soc. Edinburgh **76**, 115 (1985).
[22] S. Jana, S. H. Um, and S. Jung, Paramecium swimming in capillary tube, Phys. Fluids. **24**, 041901 (2012).
[23] A. G. Jeffs and R. C. Holland, *Swimming Behaviour of the Puerulus of the Spiny Lobster, Jasus Edwardsii (Hutton, 1875) (Decapoda, Palinuridae)* (Crustaceana, 2000), pp. 847–856.
[24] Y. Katsu-Kimura, F. Nakaya, S. A. Baba, and Y. Mogami, Substantial energy expenditure for locomotion in ciliates verified by means of simultaneous measurement of oxygen consumption rate and swimming speed, J. Exp. Biol. **212**, 1819 (2009).
[25] T. Kiørboe, A. Andersen, V. J. Langlois, and H. H. Jakobsen, Unsteady motion: Escape jumps in planktonic copepods, their kinematics and energetics, J. R. Soc., Interface. **7**, 1591 (2010).
[26] K. Kohlhage and J. Yager, An analysis of swimming in remipede crustaceans, Philos. Trans. R. Soc. London, Ser. B: Biol. Sci. **346**, 213 (1994).
[27] E. I. Lamont and R. B. Emlet, Swimming kinematics of cyprids of the barnacle *Balanus glandula*, Integr. Comp. Biol. **61**, 1567 (2021).
[28] P. H. Lenz, D. Takagi, and D. K. Hartline, Choreographed swimming of copepod nauplii, J. R. Soc., Interface. **12**, 20150776 (2015).
[29] G. Matsumoto, Swimming movements of ctenophores, and the mechanics of propulsion by ctene rows, Hydrobiologia **216**, 319 (1991).
[30] M. Morris, K. Kohlhage, and G. Gust, Mechanics and energetics of swimming in the small *copepodAcanthocyclops robustus* (Cyclopoida), Mar. Biol. **107**, 83 (1990).
[31] D. Murphy, D. Webster, S. Kawaguchi, R. King, and J. Yen, Metachronal swimming in Antarctic krill: Gait kinematics and system design, Mar. Biol. **158**, 2541 (2011).
[32] M. Ruszczyk, D. R. Webster, and J. Yen, Dual phase-shifted ipsilateral metachrony in *Americamysis bahia*, Integr. Comp. Biol. **61**, 1644 (2021).
[33] J. L. Wilkin and A. G. Jeffs, Energetics of swimming to shore in the puerulus stage of a spiny lobster: Can a postlarval lobster afford the cost of crossing the continental shelf? Limnol. Oceanogr: Fluids Environ. **1**, 163 (2011).
[34] J. Wong, B. K. Chan, and K. K. Chan, Swimming kinematics and hydrodynamics of barnacle larvae throughout development, Proc. R. Soc. B. **287**, 20201360 (2020).
[35] T. Kiørboe, H. Jiang, R. J. Gonçalves, L. T. Nielsen, and N. Wadhwa, Flow disturbances generated by feeding and swimming zooplankton, Proc. Natl. Acad. Sci. **111**, 11738 (2014).
[36] A. Skipper, D. Murphy, and D. Webster, Characterization of hop-and-sink daphniid locomotion, J. Plankton Res. **41**, 142 (2019).
[37] T. A. Williams, A model of rowing propulsion and the ontogeny of locomotion in Artemia larvae, Biol. Bull. **187**, 164 (1994).
[38] R. E. Zaret and W. C. Kerfoot, The shape and swimming technique of Bosmina longirostris 1, Limnol. Oceanogr. **25**, 126 (1980).
[39] See Supplemental Material at http://link.aps.org/supplemental/10.1103/PhysRevFluids.9.L111101 for the

spreadsheet with collected kinematics data and calculated parameters such as Reynolds and Swimming numbers for metachronal and single-pair appendage swimmers.

[40] A. Herrera-Amaya, E. K. Seber, D. W. Murphy, W. L. Patry, T. S. Knowles, M. M. Bubel *et al.*, Spatiotemporal asymmetry in metachronal rowing at intermediate Reynolds numbers, Integr. Comp. Biol. **61**, 1579 (2021).

[41] A.-M. Tassin, M. Lemullois, and A. Aubusson-Fleury, Paramecium *tetraurelia* basal body structure, Cilia. **5**, 6 (2015).

[42] J. Torres, Relationship of oxygen consumption to swimming speed in Euphausia pacifica: II. Drag, efficiency and a comparison with other swimming organisms, Mar. Biol. **78**, 231 (1984).

[43] S. P. Colin, J. H. Costello, K. R. Sutherland, B. J. Gemmell, J. O. Dabiri, and K. T. Du Clos, The role of suction thrust in the metachronal paddles of swimming invertebrates, Sci. Rep. **10**, 17790 (2020).

[44] B. D. Clark and W. Bemis, Kinematics of swimming of penguins at the Detroit Zoo, J. Zool. **188**, 411 (1979).

[45] P. Maszczyk and T. Brzezinski, Body size, maturation size, and growth rate of crustaceans, Nat. Hist. Crustacea. **5**, 35 (2018).

[46] M. P. Ford and A. Santhanakrishnan, Closer appendage spacing augments metachronal swimming speed by promoting tip vortex interactions, Integr. Comp. Biol. **61**, 1608 (2021).

[47] F.-O. Lehmann, S. P. Sane, and M. Dickinson, The aerodynamic effects of wing–wing interaction in flapping insect wings, J. Exp. Biol. **208**, 3075 (2005).

[48] X. Cheng and M. Sun, Very small insects use novel wing flapping and drag principle to generate the weight-supporting vertical force, J. Fluid Mech. **855**, 646 (2018).

[49] L. Li, M. Nagy, J. M. Graving, J. Bak-Coleman, G. Xie, and I. D. Couzin, Vortex phase matching as a strategy for schooling in robots and in fish, Nat. Commun. **11**, 5408 (2020).

[50] D. W. Murphy, D. R. Webster, and J. Yen, The hydrodynamics of hovering in Antarctic krill, Limnol. Oceanogr.: Fluids Environ. **3**, 240 (2013).

[51] G. K. Taylor, R. L. Nudds, and A. L. Thomas, Flying and swimming animals cruise at a Strouhal number tuned for high power efficiency, Nature (London). **425**, 707 (2003).

[52] G. S. Triantafyllou, M. S. Triantafyllou, and M. A. Grosenbaugh, Optimal thrust development in oscillating foils with application to fish propulsion, J. Fluids Struct. **7**, 205 (1993).

[53] M. L. Byron, D. W. Murphy, K. Katija, A. P. Hoover, J. Daniels, K. Garayev *et al.*, Metachronal motion across scales: Current challenges and future directions, Integr. Comp. Biol. **61**, 1674 (2021).

[54] R. Hayashi and D. Takagi, Metachronal swimming with rigid arms near boundaries, Fluids. **5**, 24 (2020).